

ORIGINAL RESEARCH

Association of Different Types of Osteoarthritis with Different Immune-Related Subtypes and Hub Genes

Weigang Jiang, MD; Tianyang Li, MD; Zhenzhou Tang, MD; Sucheng Li, MD; Minhua Lu, MD

ABSTRACT

Background • Osteoarthritis (OA) is a diverse disorder that most frequently affects elderly people and makes them disabled. Many investigations have shown that the etiology of OA depends on cartilage wear, but immunology also plays a significant role. Thus, the goal of this study was to define the immune-related etiology of OA.

Methods • Data from the “Gene Expression Omnibus (GEO)” database were used to find differentially expressed genes (DEGs), and the “Cell-type Identification By Estimating Relative Subsets Of RNA Transcripts (CIBERSORT) algorithm” was employed to calculate the quantity of distinct immune cells. We analyzed the results to identify patient subgroups and compare major active pathways.

Results • The macrophage cell population accounts for the greatest percentage of infiltrating immune cells in OA. One hundred and twenty-two common intersection genes were identified, with the network analysis of protein-

protein interactions revealing ten hub genes related to OA, including *CXCL8*, *JUN*, *ATF3*, *DUSP1*, *PTGS2*, *IL6*, *MMP9*, *FOS*, *NFKBIA*, and *MYC*. The random forest model showed that memory-activated CD4 T cells are strongly correlated with other immune cell types, while neutrophils have the weakest correlation with other immune cell types. Violin plots showed that OA patients had a significantly larger quantity of plasma cells and resting mast cells, with a significantly smaller quantity of resting memory CD4 T cells and activated mast cells than healthy controls.

Conclusions • Two immune-related subgroups of OA were identified by semi-supervised clustering analysis of microarray data, and core genes were also determined by network analysis. A group of the immune infiltrating cells was selected by random forest analysis suggesting they are related to the pathogenesis of OA. (*Altern Ther Health Med*. [E-pub ahead of print.]

Weigang Jiang, MD; Tianyang Li, MD; Zhenzhou Tang, MD; Sucheng Li, MD; Minhua Lu, MD, Department of Orthopedics; Suzhou Dushu Lake Hospital (Dushu Lake Hospital Affiliated to Soochow University); Suzhou City, Jiang Su Province; China.

Corresponding author: Minhua Lu, MD
E-mail: lmh910307@gmail.com

INTRODUCTION

Osteoarthritis (OA) is a progressive bone and musculoskeletal disease that most usually affects the hands, hips, and knees.^{1,2} Symptoms of OA include “slowly growing joint pain, discomfort, rigidity, joint damage, decreased mobility, and structural abnormalities”.³ The increased life expectancy in modern society is anticipated to increase the prevalence and incidence of this common and frequently-occurring disease, which seriously affects people’s daily lives. The major objectives of clinical OA therapy are pain management, maintaining or enhancing joint mobility,

and improving health conditions.⁴ However, OA treatment remains relatively limited based on its pathogenesis.^{5,6}

OA can be brought on by “prior joint injury, aberrant joint or limb formation, and genetic factors”.^{1,7} Those who are overweight, engaging in work that causes high joint stress, or possess different-sized legs have a higher risk.⁸⁻¹⁰ Although the primary pathogenesis of OA is not clear, there is no doubt that inflammation plays an important role,^{3,11} with low-grade inflammation of the entire joint promoting disease progression, leading to cartilage degradation, bone remodeling, and synovial hyperplasia.¹² Increased levels of many inflammatory mediators and cytokines are recognized in, joint effusion, cartilage, and synovium in patients with OA, including IL-1, IL-6, IL-10, and TNF- α .^{13,14} For example, TNF- α induces NF- κ B/p65 signaling to promote synovitis, cartilage degeneration, and OA progression in mice.¹⁵ Although these inflammatory variables contribute to the etiology of OA, further research is needed to determine how exactly they cause damage and how they heal it, therefore, the immune microenvironment of OA is currently being explored.

Immune cells including macrophages, T cells, B cells, plasma cells, natural killer cells, and dendritic cells have been

identified in the synovium tissue of OA individuals,¹⁶⁻¹⁸ and their recruitment may contribute to OA pain through the production of allogenic factors that increase the stimulation of sensory neurons.¹⁹ “Innate lymphocytes, $\gamma\delta$ + T cells, and CD4+ T cells” have elevated IL-17 expression and contribute to senescence-related OA progression.²⁰ Together, our findings show that immunological infiltration plays a significant role in the development of OA, however, there is no research analyzing the overall role of immune cells and inflammatory factors in OA pathogenesis.

In this study, two immune-related subgroups of OA were identified by semi-supervised clustering analysis of microarray data, and core genes were also determined by network analysis. A group of immune infiltrating cells was selected by random forest analysis suggesting that they are related to the pathogenesis of OA.

MATERIALS AND METHODS

Collection of micro-array data and clinical features of data

We retrieved the gene expression data from the GSE55235 (which included 10 OA patients and 10 control individuals) and the GSE55457 (which included 10 OA patients and 10 control individuals), both based on platform GPL96²¹ from “the Gene Expression Omnibus (GEO) database (<https://www.ncbi.nlm.nih.gov/geo/>)” utilizing “GEOquery R package”²² (see Table 1 for details). The affy R package from Bioconductor was used to extract raw Affymetrix CEL files and normalize them using the “robust multi-array analysis (RMA) algorithm” technique.²³ The normalization procedure was performed separately for each data set and log₂-transformed values by RMA were used to present gene expression levels. Those genes that had a value of expression of more than one were retained, and the less abundant data were disqualified. A gene expression profile matrix was created by using the average probe expression for numerous probes referring to a single gene as the gene expression value. Batch effects correction was performed by the sva R package²⁴ and visualized in a boxplot using the ggplot² R package.²⁵

The relationship between immune cell type and OA

Depending on complicated tissues’ gene expression profiles, the “CIBERSORT method” is frequently utilized to predict the “immune cell component” and quantity,^{26,27} and is shown to perform better than conventional techniques.²⁸ This study determined the proportion of immune cells in the OA patients using “CIBERSORT and the LM22 signature” from the microarray data, demonstrating that LM22, a leukocyte gene signature matrix of 547 genes, can discriminate 22 different types of immune cells.²⁶ First, the normalized gene expression matrix was uploaded into CIBERSORT using the LM22 gene signature and then run for 1000 permutations. The result was a *P* value which shows deconvolution in each of the samples and a threshold of *P* less than 0.05 was included for identifying the immune infiltration matrix. The distribution of 22 different immune

Table 1. Details of Datasets GSE55235 and GSE55457

ID	Platform	Number of case	Number of control	Sample source	Species
GSE 55235	GPL96	10 OA	10 control	Synovial tissue	Homo sapiens
GSE 55457	GPL96	10 OA	10 control	Synovial tissue	Homo sapiens

cell types in each specimen was displayed using the “heatmap R package” (available at <https://CRAN.R-project.org/package=heatmap>), and the relationship between immune cell types was presented using the “copilot R program”.²⁹

Consensus cluster and differentially expressed gene (DEGs) analysis

Unsupervised clustering of the OA patient samples was performed with the “ConsensusClusterPlus R package”³⁰ using the topmost variable genes to confirm the optimum number of clusters with the gene expression profile. The relative change under the area of the distribution curve determined the number of clusters. Using the limma R tools,³¹ DEGs were found, and those with an absolute log₂ fold change larger than 1 and an adjusted *P* < .05 were filtered out. Using the ggplot2 R tool, a volcano plot and heatmap of DEGs were constructed.²⁵

Weighted correlation network analysis (WGCNA)

WGCNA was performed using the “WGCNA R package” following the gene co-expression patterns to investigate the gene co-regulatory network in OA patients.³² To create a topological overlap matrix from the gene correlation network, the power parameter was chosen. The dynamic hybrid cut was used to identify closely interconnected modules, and the module with the biggest difference was evaluated.

Enrichment Analysis

We carried out “Gene Ontology (GO)³³ and KEGG³⁴ pathway analysis of immune genes” using the “clusterProfiler R package”.³⁵ The “enrich plot R program” was used to display significant GO biological processes (false discovery rate (FDR) less than 0.05). To determine which biological processes are assisting the OA clusters, the clusterProfiler R package was used to perform “gene set enrichment analysis (GSEA)”³⁵ with GO gene sets (C2) from the “Molecular Signature Database (MSigDB; version 6.1)”.³⁶ The gene expression matrix of OA and control samples were used as input data for one thousand permutations, and significant results were defined as having an FDR *q*-value of less than 0.25 and *P* < .05.

Construction and investigation of Protein-protein interaction (PPI) network

We utilized the “STRING database”^{37,38} for analyzing the PPI relationship of DEGs related to OA. The DEGs were uploaded into the STRING database and the PPIs were downloaded from the website. Only interactors with a medium combined confidence score greater than 0.4 were retained. Then, Cytoscape was used to carefully monitor the whole network.³⁹ The hub genes inside the PPI network were discovered using the Cytoscape plugins cytoHubba and

ClusterViz according to the degree of connectedness.³⁹ The top 10 hub genes with greater Maximal Clique Centrality (MCC) values were shown by the node degree.

The immune model

To study the main immune cell types involved in OA, we constructed an immune-related model based on the “random forest R package”⁴⁰ The “stepwise backward selection method” was used to determine the best combination of recursive prediction candidate modules. 10 percent of the characteristics were removed in each iteration, with the remaining features used to construct the random forest model. A variable selection technique known as backward stepwise selection (or backward elimination) starts with a model that includes all variables being considered (referred to as the Full Model) and commences trying to remove the least relevant variables one at a time until a pre-determined stopping rule has arrived or there are no more variables in the model. The relationship between each hub gene and the important immune cells in the immunological model was examined using the “ggpubr R package” (<https://CRAN.R-project.org/package=ggpubr>).

Statistical analysis

For data acquisition and quantitative models, R software (version 3.6.5, <http://r-project.org/>) was utilized. Independent *t* tests were used to determine the significance of normally distributed continuous variables. Non-normally distributed continuous variables were subjected to the Mann-Whitney U test. The association between various genes was compared using the Pearson correlation. The statistical *P* values were two-sided, and statistical significance was set at *P* < .05.

RESULTS

Data Progress and Quality Control

First, raw data from GSE55235 and GSE55457 were preprocessed and normalized separately. Boxplot diagrams and PCA plots (Figures 1A and 1B) before and after (Figures 1C and 1D) the batch correction showed that the batch was well removed, and that data can be combined for downstream analysis.

Immune infiltration landscape between OA patients and healthy controls

In the OA group, Figure 2A depicts the distribution of “22 immune cells,” with the macrophage cell population being in charge of the majority of the infiltrating immune cells. The “Correlation analysis” was performed between distinct immune cells to examine the correlation between the groups (Figure 2B). Among them, memory-activated CD4 T cells strongly correlated with other immune cell types, while neutrophils have the weakest correlation with other immune cell types. Violin plots showed that OA patients had a significantly larger quantity of plasma cells and resting mast cells, with a significantly smaller quantity of resting memory CD4 T cells and activated mast cells than the healthy control (Figure 2C).

Figure 1. Distribution of GSE55235 and GSE55457 Data Before and After Batch Correction. (A) Boxplot of GSE55235 and GSE55457 Datasets Before Batch Correction; (B) Boxplot of GSE55235 and GSE55457 Datasets After Batch Correction; (C) PCA Plot of GSE55235 and GSE55457 Datasets Before Batch Correction; (D) PCA Plot of GSE55235 and GSE55457 Datasets After Batch Correction.

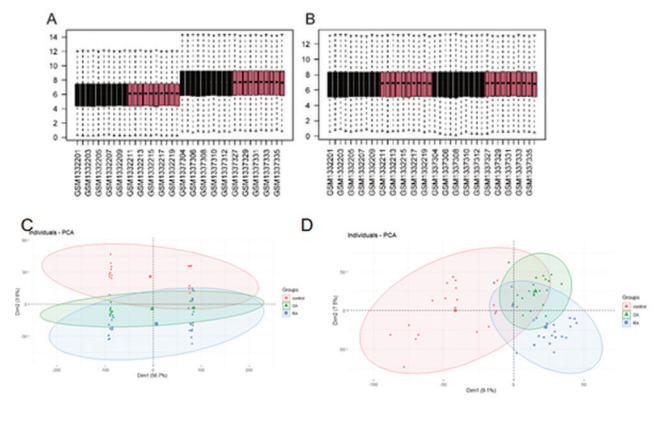
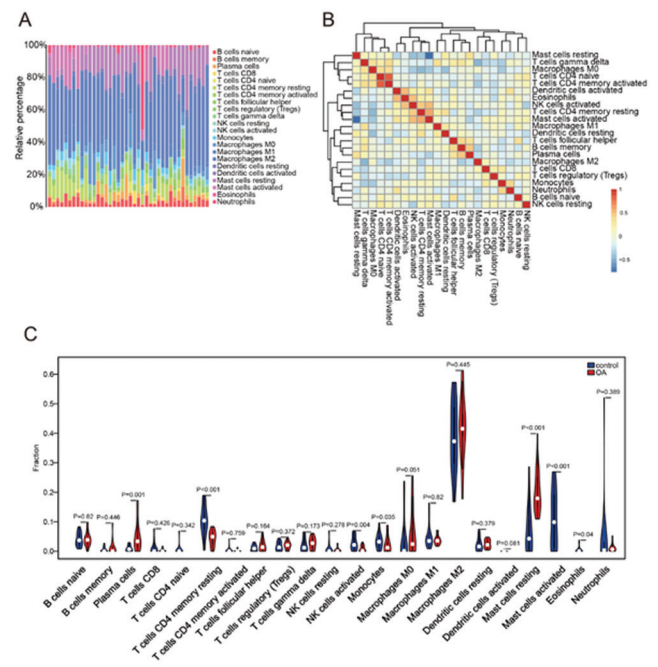


Figure 2. Distribution of Immune Cell Infiltration in OA Samples. (A) Bar Chart of the Proportion of 22 Immune Cell Types According to the CIBERSORT Algorithm; (B) Correlation of 22 Immune Cell Types, Blue Indicates a Positive Correlation and Red Indicates a Negative Correlation; (C) Differential Expressed Immune Cell Types in the OA Versus Control Groups.



The construction of immune-related subtypes in OA patients

To unravel the immune characteristics of OA patients, we applied consensus clustering of immune-related genes and divided the OA patients into two sub-clusters (Figure 3A). Gene expression profiles of the two clusters were compared, and the results identified 132 DEGs (FDR<0.05

Figure 3. Consensus Clustering of Gene Expression Profiles Identifies Two Major Clusters. (A) Heatmap of Consensus Scores; (B) Heatmap of the Consensus Clustering Using the Top 20 and Bottom 20 Genes with the Most Differences; (C) The Volcano Plot of All the Genes Between OA Group and the Control Group; Red Represents Upregulated Genes, Blue Represents Downregulated Genes, and Gray Represents Stable Genes.

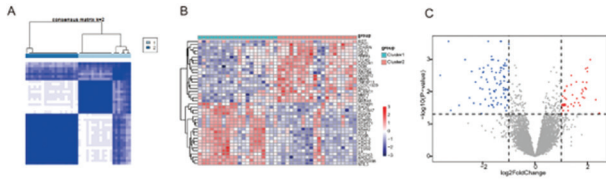
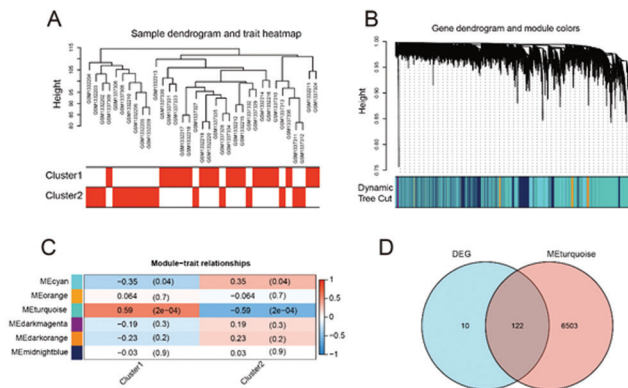


Figure 4. WGCNA Analysis Based on the Two Major Clusters. (A) Sample Dendrogram and Trait Heatmap; (B) Gene Dendrogram and Module Scores; (C) WGCNA Correlation With Clinical Variables; (D) Venn Diagram Showing the Common Genes for the MEturquoise Subgroups and Differential Genes.



and $|\log_2 \text{fold change}| > 2$). Among them, the heatmap of the top 20 and the bottom 20 genes showed good separation of the two clusters (Figure 3B). All genes were visualized in a volcano plot and significant differential genes were highlighted, gray indicates unresponsive genes, blue indicates differential genes that are downregulated, and red indicates differential genes that are upregulated (Figure 3C).

WGCNA analysis based on immune-related subtypes

Next, we conducted WGCNA analysis based on immune cell subpopulations showing that genes from MEturquoise subpopulations were the most significant (Figure 4A-C). We then intersected genes from MEturquoise with DEGs calculated between cluster 1 and cluster 2, showing there are 122 common intersection genes (Figure 4D).

Functional Enrichment Analysis

To learn more about the fundamental biochemical pathways and GO physiological functions of immune-related genes, functional enrichment screening was used. GO investigation revealed that 122 genes are critically related to the cell chemotaxis, collagen-containing extracellular matrix, regulation of inflammatory response, negative

Figure 5. GO and KEGG Enrichment Analysis. (A) GO Enrichment Analysis. The X-Axis Represents the Proportion of DEGs Enriched in GO Term, the Color of the Dot Represents the Corrected P-Value and the Length of the Axis Represents the Number of Enriched Genes; (B) GO Enrichment Analysis Network Diagram; (C) KEGG Pathway Enrichment Analysis. The X-Axis Represents the Proportion of DEGs Enriched in the KEGG Term, the Color of the Dot Represents the Corrected P-Value and the Length of the Axis Represents the Number of Enriched Genes; (D) KEGG Enrichment Analysis Network Diagram.

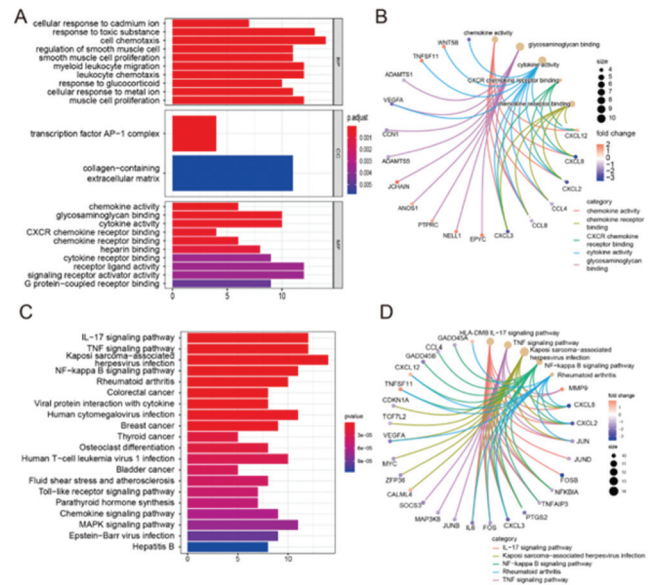
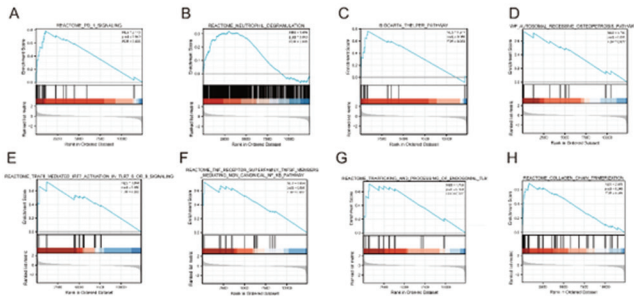


Table 2. KEGG Enrichment Result

ID	Description	P adjust	q-value	Count
hsa05167	Kaposi sarcoma-associated herpesvirus infection	1.19E-07	7.42E-08	14
hsa04657	IL-17 signaling pathway	8.75E-09	5.47E-09	12
hsa04668	TNF signaling pathway	3.55E-08	2.22E-08	12
hsa04064	NF-kappa B signaling pathway	1.19E-07	7.42E-08	11
hsa05163	Human cytomegalovirus	0.0001601	0.0001001	11
hsa04010	MAPK signaling pathway	0.0008603	0.0005382	11
hsa05323	Rheumatoid arthritis	4.59E-07	2.87E-07	10
hsa05166	Human T-cell leukemia virus 1	0.0005307	0.000332	10
hsa05224	Breast cancer	0.000177	0.0001107	9
hsa04062	Chemokine signaling pathway	0.0007887	0.0004935	9
hsa05169	Epstein-Barr virus infection	0.001045	0.0006538	9
hsa05417	Lipid and atherosclerosis	0.0015221	0.0009523	9
hsa05132	Saimonella infection	0.0029804	0.0018646	9
hsa04060	Cytokine-cytokine receptor interaction	0.0079814	0.0049933	9
hsa05210	Colorectal cancer	3.85E-05	2.41E-05	8
hsa04061	Viral protein interaction wth cytokine and cytokine receptor	0.0001044	6.53E-05	8
hsa04380	Osteoclast differentiation	0.0004151	0.0002597	8
hsa05418	Fluid shear stress and atherosclerosis	0.0005921	0.0003704	8
hsa05161	Hepatitis B	0.0012261	0.0007671	8
hsa04621	NOD-like receptor signaling path way	0.0022661	0.0014177	8
hsa05202	Transcriptional misregulation in cancer	0.0027121	0.0016967	8
hsa05207	Chemical carcinogenesis-receptor activation	0.0041093	0.0025708	8

regulation of protein phosphorylation, regulation of vasculature development, negative regulation of phosphorylation, and receptor-ligand activity (Figure 5A-B) (Table S1). The KEGG enrichment results of the 122 genes are shown in Figure 5C-D. The pathways enriched in the KEGG database are mainly related to “Kaposi sarcoma-associated herpesvirus infection, IL-17 signaling pathway, TNF signaling pathway, NF-kappa B signaling pathway, and human cytomegalovirus infection” (Table 2).

Figure 6. GSEA Enrichment Analysis of the Top Eight Pathways Showing that OA is Closely Related to PD-1 Signaling (A), Neutrophil Degranulation (B), the Biocarta T-helper Pathway (C), Autosomal Recessive Osteopetrosis Pathways (D), TRAF6 Mediated IRF7 Activation in TLR7 8 or 9 Signaling (E), TNF Receptor Superfamily TNFSF Members Mediating the Non-Canonical NF-kB Pathway (F), Trafficking and Processing of Endosomal TLR (G), and Collagen Chain Trimerization (H).



GSEA analysis revealed that pathways related to Reactome PD-1 signaling (Figure 6A), Reactome neutrophil degranulation (Figure 6B), Biocarta T-helper pathway (Figure 6C), WP autosomal recessive osteopetrosis pathways (Figure 6D), “Reactome TRAF6 mediated IRF7 activation in TLR7 8 or 9 signalings” (Figure 6E), “Reactome TNF receptor superfamily TNFSF members mediating non -canonical NF-kB pathway” (Figure 6F), “Reactome trafficking and processing of endosomal TLR” (Figure 6G), and “Reactome collagen chain trimerization” (Figure 6H) were significantly upregulated in cluster 1 (Table 3).

Analysis of the PPI Network

Hub nodes play an important role in the biological network, therefore, the PPI relationship of DEGs with different immune-related clusters of OA patients was investigated. The full PPI network is shown in Figure 7A, with genes colored and classified according to the up and down levels (Figure 7B). The top 10 hub genes, such as CXCL8, JUN, ATF3, DUSP1, PTGS2, IL6, MMP9, FOS, NFKBIA, and MYC were determined by computing the MCC values (Figure 7C).

Integration of a random forest model based on immune cells and hub gene

Several decision trees are combined to create a Random Forest, which makes more precise predictions. The rationale is that numerous uncorrelated models (the individual decision trees) perform better together than they do individually. To further refine the immune-related genes, a “random forest model” was built based on OA patients, composed of the 22 immune cells (Figure 8A-B), showing that activated “NK cells, resting memory CD4 T cells, resting mast cells, activated mast cells, M0 macrophages, M1 macrophages, plasma cells, and naïve B cells” are the crucial immunological cells associated with the pathogenesis of OA.

Table 3. GSEA Enrichment Result

ID	enrichmentScore	NES	p.adjust
REACTOME_PD_1_SIGNALING	0.825817	2.172937	8.71E-05
REACTOME_PHOSPHORYLATION_OF_CD3_AND_TCR_ZETA_CHAI	0.821882	2.127981	0.000101
REACTOME_TRANSLOCATION_OF_ZAP_70_TO_IMMUNOLOGICAL	0.794383	1.990149	0.001157
WILENSKY_RESPONSE_TO_DARAPLADIB	0.791084	2.375836	1.31E-06
GUTIERREZ_CHRONIC_LYMPHOCYtic_LEUKEMIA_UP	0.783268	1.917542	0.003916
GOERING_BLOOD_HDL_CHOLESTEROL_QTL_CIS	0.772096	1.815714	0.020032
BIOCARTA_THELPER_PATHWAY	0.76344	1.868999	0.008003
HAHTOLA_CTCL_PATHOGENESIS	0.753092	1.949634	0.002708
GRAHAM_CML_QUIESCENT_VS_NORMAL_DIVIDING_DN	0.749	1.83366	0.012455
FARMER_BREAST_CANCER_CLUSTER_1	0.744857	2.482431	4.04E-08
BIOCARTA_TORA_PATHWAY	0.737953	1.763317	0.022131
ANASTASSIOU_MULTICANCER_INVASIVENESS_SIGNATURE	0.736273	2.694588	7.60E-09

Figure 7. Protein-Protein Interaction (PPI) Analysis. (A) PPI Network Analysis, Red Represents High Expression and Blue Represents Low Expression; (B) Protein Cluster Analysis, Yellow or Pink Represent a Cluster; (C) Hub Genes Prediction, Red Represents the Hub Gene.

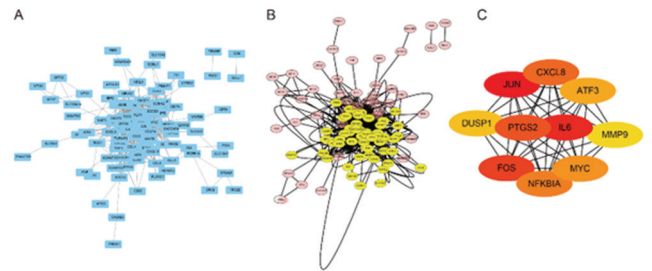


Figure 8. The Construction of an Immune Model Based on the Hub Gene and Immune Cells. (A–B) Random Forest Analysis Results Show that T cell and Master Cell Subgroups Account for a Large Proportion of Infiltrating Immune Cells; (C–R) The Correlation of Hub Genes and the Main Immune Cell Types.

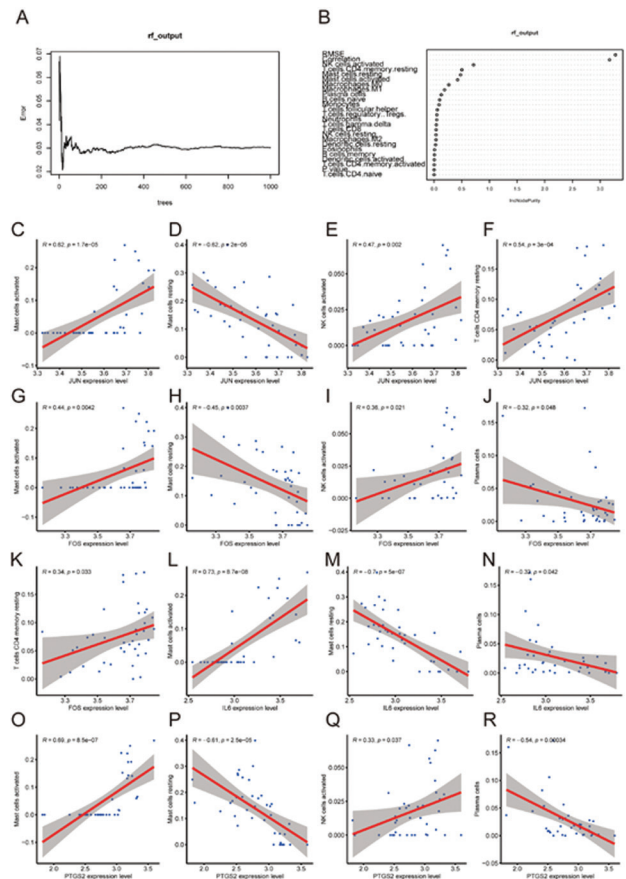


Figure 8C-R displays the relationship between the various hub genes and the key immunological cells, illuminating the superiority of the random forest model for OA-associated factor prediction.

DISCUSSION

For the projection of the responsiveness and pathophysiology of OA, it is crucial to comprehend the link between immune infiltration and fundamental genes. Infiltrated immune cells including macrophages, T and B cells, mast cells, plasma cells, natural killer cells, dendritic cells, and granulocytes were found inside the synovium of OA patients.^{41,42} Synovial swelling, subchondral bone sclerosis, and the development of osteophytes are all caused by the production of cytokines and chemokines by T lymphocytes, B lymphocytes, and macrophages that have invaded the articular cavity.⁴³ Although the inflammation caused by these immune cells is low-level and chronic, it causes serious joint damage, and its pathogenesis needs to be studied.

Macrophages are associated with the pathophysiology of OA, including cartilage breakdown, synovial inflammatory activities, and subchondral bone damage, as an essential effector cell in the initial stage of inflammatory destruction.^{17, 44, 45} Up to 90% of patients with end-stage OA have a large number of macrophages infiltrating the synovium,⁴⁶ therefore macrophages are closely related to the pathogenesis of OA. Herein, we investigated infiltrated immune cell types in OA by exploring microarray data from the GEO database, demonstrating that the majority of immune cells that infiltrate OA are composed of the macrophage subpopulation. By secreting different inflammatory factors, macrophages played important role in the inflammatory disease and OA.⁴⁷ For example, the inhibition of autophagy in macrophages promotes the release of mature IL-1 β , which contributes to the occurrence of synovitis and OA.⁴⁸ Advances in understanding macrophage recruitment and activation provide opportunities for OA therapies.

One of the major results of the study was that the pattern of gene expression in OA falls into two clear clusters, which have 122 common intersection genes mainly enriched in “cell chemotaxis, collagen-containing extracellular matrix, regulation of inflammatory response, negative regulation of protein phosphorylation, regulation of vasculature development, negative regulation of phosphorylation, receptor-ligand activity, IL-17 signaling pathway, TNF signaling pathway, and NF-kappa B signaling pathway”. OA pathogenesis depends to a large extent on the imbalance of proinflammatory and anti-inflammatory mediators,⁴⁹ and the activation of signaling pathways of NF- κ B also activates other mechanisms that may promote OA progression. Similarly, the NF- κ B signaling pathway may contribute to the occurrence of OA.⁵⁰ IL-17 is involved in inducing and mediating proinflammatory responses and blocking the IL-17 signaling pathway can delay OA-related pain.⁵¹

Ten hub nodes were identified including *CXCL8*, *JUN*, *ATF3*, *DUSP1*, *PTGS2*, *IL6*, *MMP9*, *FOS*, *NFKBIA*, and

MYC. A minor chemokine from the C-X-C motif (CXC) family amongst them called CXCL8 promotes the release of inflammatory cytokines, thus further controlling the inflammatory process.⁵² The increased expression of CXCL8 facilitates the activation and migration of human lymphocytes from vessels to the joint tissues via the CXC chemokine pathway. The JUN protein is a type of activated protein-1 (AP-1) transcription complex that is intimately associated with the development of OA. The JNK/c-JUN pathway promoted chondrocyte apoptosis in an OA model induced by IL-1 β ⁵³ and the homozygous genotype of FOS promoter single nucleotide polymorphisms (SNP) is associated with the susceptibility for knee OA.⁵⁴ Furthermore, during OA, the JNK-c-JUN pathway plays a role in the overexpression of Bim.⁵⁵ Leucine zipper-shaped activating transcription factor 3 (ATF3), a member of the ATF/CREB family of transcription factors, is quickly triggered by a string of harmful stress signals. By controlling the expression of inflammatory cytokines in chondrocytes, ATF3 is a crucial mediator in the formation and progression of OA; as a result, cytokines/NF- κ B/Atf3 in chondrocytes may be a promising target for OA therapy.⁵⁶

Among the ten hub nodes, dual specific phosphatase 1 (DUSP1) regulates the transduction of MAPK, c-JUN, and MYC signal pathways via the dephosphorylation activity of threonine, serine, and tyrosine. In synovial biopsies taken from people with rheumatoid arthritis and osteoarthritis, DUSP1 is dysregulated,⁵⁷ indicating its involvement in the pathogenesis of OA. Downregulation of DUSP1 inactivates MAPK, p38, and JNK signals, leading to an increased expression of RANKL and severe bone destruction in patients with OA.⁵⁸ Prostaglandin endoperoxide synthase 2 (PTGS2) is induced by extracellular stimuli to regulate inflammation and repress the expression of COX-2; Hip and knee OA are related to a reduced risk due to COX-2, which is linked to the decreased risk of hip and knee OA.⁵⁹ TNF- α , MMP-2, MMP-8, and COX-2 expression increased in the IL-1-induced rat OA model, showing that PTGS2 mediates the expression of COX-2 and MMPs family proteins essential for the development of OA.⁶⁰ The etiology of OA could also be linked to the higher production of MMP-9 molecules.⁶¹ IL6 is a key proinflammatory cytokine and the most prominently elevated cytokine in the synovial fluid of OA individuals.⁶² IL-6 induced STAT3 and ERK1/2 signalling in a mouse OA model, and MMP-3 and MMP-13 levels were elevated for promoting chondrocyte apoptosis.⁶³

IL-1 β , which is an OA master regulator, stimulates the production of IL-6, which in turn causes the “initiation, phosphorylation, and DNA binding capability of c-FOS” (one of the main components of AP).⁶⁴ For patients with OA, the high expression of FOS predicts high pain and inflammation.⁶⁵ The *NFKBIA* gene encodes the I κ B α protein in the NF- κ B complex, and its SNP characteristics can help assess the risk of OA patients.⁶⁶ The expression of c-MYC is positively correlated with chondrocyte apoptosis and cartilage destruction and is a hub gene for OA development.^{67,68} These results revealed the importance of core genes in the development of OA, which is consistent with our data.

Finally, a random forest model was created using OA patients' selection of a set of immune infiltrating cell types following additional examination of the 22 immune cell types. It is to be noted that, "activated NK cells, resting memory T cells CD4, resting mast cells, activated mast cells, M0 macrophages, M1 macrophages, plasma cells, and naïve B cells" are the main immune cells involved in OA.^{16,67} These cell types correlated well with the hub genes indicating that the random forest model had remarkable power for predicting different clinical procedures.

Although high-throughput microarray data from the GEO databases were utilized to investigate the immune landscape of OA, the present study has some limitations. The entire study was conducted retrospectively, and the findings are derived from a single platform. It is necessary to obtain data from different platforms, and functional experiments are to be performed to monitor the functions of these markers at the molecular level.

CONCLUSION

OA patients had a significantly larger quantity of plasma cells and resting mast cells than healthy controls. Pathway analysis showed that the genes related to OA specifically include "immune responses and immune-associated signaling pathways, such as the IL-17 signaling pathway and NF-kappa B signaling pathway". In addition, a group of immune infiltrating cells related to OA was selected, which helped to understand the pathogenesis of OA.

AUTHOR DISCLOSURE STATEMENT

The authors declare that they have no competing interests.

FUNDING

There was no financial support of any kind provided for this research.

ACKNOWLEDGEMENT

Weigang Jiang and Tianyang Li contributed equally to this work.

DATA AVAILABILITY

On request, the corresponding author will provide access to the data that supported this work.

REFERENCES

- Glyn-Jones S, Palmer AJ, Agricola R, et al. Osteoarthritis. *Lancet*. 2015;386(9991):376-387. doi:10.1016/S0140-6736(14)60802-3
- Mathiessen A, Conaghan PG. Synovitis in osteoarthritis: current understanding with therapeutic implications. *Arthritis Res Ther*. 2017;19(1):18. doi:10.1186/s13075-017-1229-9
- Chen D, Shen J, Zhao W, et al. Osteoarthritis: toward a comprehensive understanding of pathological mechanism. *Bone Res*. 2017;5(1):16044. doi:10.1038/boneres.2016.44
- Ratneswaran A, Rockel JS, Kapoor M. Understanding osteoarthritis pathogenesis: a multiomics system-based approach. *Curr Opin Rheumatol*. 2020;32(1):80-91. doi:10.1097/BOR.0000000000000680
- Lane NE, Shidara K, Wise BL. Osteoarthritis year in review 2016: clinical. *Osteoarthritis Cartilage*. 2017;25(2):209-215. doi:10.1016/j.joca.2016.09.025
- Abramoff B, Caldera FE. Osteoarthritis: Pathology, Diagnosis, and Treatment Options. *Med Clin North Am*. 2020;104(2):293-311. doi:10.1016/j.mcna.2019.10.007
- Osteoarthritis BR. *Lancet*. 2018;391(10134):1985. doi:10.1016/S0140-6736(18)31064-X
- Berenbaum F. Osteoarthritis as an inflammatory disease (osteoarthritis is not osteoarthrosis!). *Osteoarthritis Cartilage*. 2013;21(1):16-21. doi:10.1016/j.joca.2012.11.012
- Issa RI, Griffin TM. Pathobiology of obesity and osteoarthritis: integrating biomechanics and inflammation. *Pathobiol Aging Age Relat Dis*. 2012;2(2012). doi:10.3402/pba.v2i0.17470
- Veenhof C, Huisman PA, Barten JA, Takken T, Pisters MF. Factors associated with physical activity in patients with osteoarthritis of the hip or knee: a systematic review. *Osteoarthritis Cartilage*. 2012;20(1):6-12. doi:10.1016/j.joca.2011.10.006
- Orlowsky EW, Kraus VB. The role of innate immunity in osteoarthritis: when our first line of defense goes on the offensive. *J Rheumatol*. 2015;42(3):363-371. doi:10.3899/jrheum.140382
- Sokol CL, Luster AD. The chemokine system in innate immunity. *Cold Spring Harb Perspect Biol*. 2015;7(5):a016303. doi:10.1101/cshperspect.a016303
- Woodell-May JE, Sommerfeld SD. Role of Inflammation and the Immune System in the Progression of Osteoarthritis. *Journal of orthopaedic research : official publication of the Orthopaedic Research Society*. 2020;38(2):253-257. doi:10.1002/jor.24457
- Wojdasiewicz P, Poniatowski L A, Szukiewicz D. The role of inflammatory and anti-inflammatory cytokines in the pathogenesis of osteoarthritis. *Mediators of inflammation*. 2014;2014(2014):561459. doi:10.1155/2014/561459

- Chen Z, Lin CX, Song B, et al. Spermidine activates RIP1 deubiquitination to inhibit TNF- α -induced NF- κ B/p65 signaling pathway in osteoarthritis. *Cell Death Dis*. 2020;11(7):503. doi:10.1038/s41419-020-2710-y
- Wu X, Lu W, Xu C, et al. Macrophages Phenotype Regulated by IL-6 Are Associated with the Prognosis of Platinum-Resistant Serous Ovarian Cancer: Integrated Analysis of Clinical Trial and Omics. *J Immunol Res*. 2023;2023:6455704. doi:10.1155/2023/6455704
- Zhang H, Cai D, Bai X. Macrophages regulate the progression of osteoarthritis. *Osteoarthritis Cartilage*. 2020;28(5):555-561. doi:10.1016/j.joca.2020.01.007
- Weber A, Chan PMB, Wen C. Do immune cells lead the way in subchondral bone disturbance in osteoarthritis? *Prog Biophys Mol Biol*. 2019;148:21-31. doi:10.1016/j.pbmolbio.2017.12.004
- Miller RJ, Malfait AM, Miller RE. The innate immune response as a mediator of osteoarthritis pain. *Osteoarthritis Cartilage*. 2020;28(5):562-571. doi:10.1016/j.joca.2019.11.006
- Faust HJ, Zhang H, Han J, et al. IL-17 and immunologically induced senescence regulate response to injury in osteoarthritis. *J Clin Invest*. 2020;130(10):5493-5507. doi:10.1172/JCI134091
- Woetzel D, Huber R, Kupfer P, et al. Identification of rheumatoid arthritis and osteoarthritis patients by transcriptome-based rule set generation. *Arthritis Res Ther*. 2014;16(2):R84. doi:10.1186/ar4526
- Davis S, Meltzer PS. GEOquery: a bridge between the Gene Expression Omnibus (GEO) and BioConductor. *Bioinformatics*. 2007;23(14):1846-1847. doi:10.1093/bioinformatics/btm254
- Gautier L, Cope L, Bolstad BM, Irizarry RA. affy-analysis of Affymetrix GeneChip data at the probe level. *Bioinformatics*. 2004;20(3):307-315. doi:10.1093/bioinformatics/btg405
- Leek JT, Johnson WE, Parker HS, Jaffe AE, Storey JD. The sva package for removing batch effects and other unwanted variation in high-throughput experiments. *Bioinformatics*. 2012;28(6):882-883. doi:10.1093/bioinformatics/bts034
- Pearson GS. Reviewing Manuscripts With Problematic Language Issues. *J Am Psychiatr Nurses Assoc*. 2019;25(4):251-252. doi:10.1177/1078390319857707
- Newman AM, Liu CL, Green MR, et al. Robust enumeration of cell subsets from tissue expression profiles. *Nat Methods*. 2015;12(5):453-457. doi:10.1038/nmeth.3337
- Ali HR, Chlon L, Pharoah PD, Markowitz F, Caldas C. Patterns of Immune Infiltration in Breast Cancer and Their Clinical Implications: A Gene-Expression-Based Retrospective Study. *PLoS Med*. 2016;13(12):e1002194. doi:10.1371/journal.pmed.1002194
- Jiang Y-Z, Ma D, Suo C, et al. Genomic and Transcriptomic Landscape of Triple-Negative Breast Cancers: Subtypes and Treatment Strategies. *Cancer Cell*. 2019;35(3):428-440.e5. doi:10.1016/j.ccell.2019.02.001
- Wei T, Simko V. R package "corrplot": Visualization of a Correlation Matrix. 2017.
- Wilkerson MD, Hayes DN. ConsensusClusterPlus: a class discovery tool with confidence assessments and item tracking. *Bioinformatics*. 2010;26(12):1572-1573. doi:10.1093/bioinformatics/btq170
- Ritchie ME, Phipson B, Wu D, et al. limma powers differential expression analyses for RNA-seq and microarray studies. *Nucleic Acids Res*. 2015;43(7):e47. doi:10.1093/nar/gkv007
- Langfelder P, Horvath S. WGCNA: an R package for weighted correlation network analysis. *BMC Bioinformatics*. 2008;9(1):559. doi:10.1186/1471-2105-9-559
- Ashburner M, Ball CA, Blake JA, et al; The Gene Ontology Consortium. Gene ontology: tool for the unification of biology. *Nat Genet*. 2000;25(1):25-29. doi:10.1038/75556
- Kanehisa M, Goto S. KEGG: kyoto encyclopedia of genes and genomes. *Nucleic Acids Res*. 2002;30(1):27-30. doi:10.1093/nar/28.1.27
- Yu G, Wang LG, Han Y, He QY. clusterProfiler: an R package for comparing biological themes among gene clusters. *OMICS*. 2012;16(5):284-287. doi:10.1089/omi.2011.0118
- Liberzon A, Subramanian A, Pinchback R, Thorvaldsdottir H, Tamayo P, Mesirov JP. Molecular signatures database (MSigDB) 3.0. *Bioinformatics*. 2011;27(12):1739-1740. doi:10.1093/bioinformatics/btr260
- Szklarczyk D, Franceschini A, Wyder S, et al. STRING v10: protein-protein interaction networks, integrated over the tree of life. *Nucleic Acids Res*. 2015;43(Database issue):D447-D452. doi:10.1093/nar/gku1003
- Szklarczyk D, Morris JH, Cook H, et al. The STRING database in 2017: quality-controlled protein-protein association networks, made broadly accessible. *Nucleic Acids Res*. 2017;45(D1):D362-D368. doi:10.1093/nar/gkw937
- Cline MS, Smoot M, Cerami E, et al. Integration of biological networks and gene expression data using Cytoscape. *Nat Protoc*. 2007;2(10):2366-2382. doi:10.1038/nprot.2007.324
- Liaw A, Wiener M. Classification and regression by randomForest. *R News*. 2002;2(3):18-22.
- Zhao X, Zhao Y, Sun X, Xing Y, Wang X, Yang Q. Immunomodulation of MSCs and MSC-Derived Extracellular Vesicles in Osteoarthritis. *Front Bioeng Biotechnol*. 2020;8:575057. doi:10.3389/fbioe.2020.575057
- Li YS, Luo W, Zhu SA, Lei GH. T Cells in Osteoarthritis: alterations and Beyond. *Front Immunol*. 2017;8:356. doi:10.3389/fimmu.2017.00356
- Robinson WH, Lepus CM, Wang Q, et al. Low-grade inflammation as a key mediator of the pathogenesis of osteoarthritis. *Nat Rev Rheumatol*. 2016;12(10):580-592. doi:10.1038/nrrheum.2016.136
- Hu W, Chen Y, Dou C, Dong S. Microenvironment in subchondral bone: predominant regulator for the treatment of osteoarthritis. *Ann Rheum Dis*. 2021;80(4):413-422. doi:10.1136/annrheumdis-2020-218089
- Griffin TM, Scanzello CR. Innate inflammation and synovial macrophages in osteoarthritis pathophysiology. *Clin Exp Rheumatol*. 2019;37 Suppl 120(5):57-63.
- Hamilton JA, Cook AD, Tak PP. Anti-colony-stimulating factor therapies for inflammatory and autoimmune diseases. *Nat Rev Drug Discov*. 2016;16(1):53-70. doi:10.1038/nrd.2016.231
- Wu CL, Harasymowicz NS, Klimak MA, Collins KH, Guilak F. The role of macrophages in osteoarthritis and cartilage repair. *Osteoarthritis Cartilage*. 2020;28(5):544-554. doi:10.1016/j.joca.2019.12.007
- Zhang B, Chen H, Ouyang J, et al. SQSTM1-dependent autophagic degradation of PKM2 inhibits the production of mature IL1 β -IL1 β and contributes to LIPUS-mediated anti-inflammatory effect. *Autophagy*. 2020;16(7):1262-1278. doi:10.1080/15548627.2019.1664705
- Molnar V, Matisić V, Kodvanj I, et al. Cytokines and Chemokines Involved in Osteoarthritis Pathogenesis. *Int J Mol Sci*. 2021;22(17):9208. doi:10.3390/ijms22179208
- Liu YX, Wang GD, Wang X, Zhang YL, Zhang TL. Effects of TLR-2/NF- κ B signaling pathway on the occurrence of degenerative knee osteoarthritis: an in vivo and in vitro study. *Oncotarget*. 2017;8(24):38602-38617. doi:10.18632/oncotarget.16199
- Liu Y, Peng H, Meng Z, Wei M. Correlation of IL-17 Level in Synovia and Severity of Knee Osteoarthritis. *Med Sci Monit*. 2015;21:1732-1736. doi:10.12659/MSM.893771
- Pierzchala AW, Kusz DJ, Hajduk G, CXCL8 and CCL5 expression in synovial fluid and blood serum in patients with osteoarthritis of the knee. *Arch Immunol Ther Exp (Warsz)*. 2011;59(2):151-155. doi:10.1007/s00005-011-0115-4
- Lu H, Hou G, Zhang Y, Dai Y, Zhao H. c-Jun transactivates Puma gene expression to promote osteoarthritis. *Mol Med Rep*. 2014;9(5):1606-1612. doi:10.3892/mmr.2014.1981
- Huber R, Kirsten H, Näkki A, et al. Association of Human FOS Promoter Variants with the Occurrence of Knee-Osteoarthritis in a Case Control Association Study. *Int J Mol Sci*. 2019;20(6):1382. doi:10.3390/ijms20061382
- Ye Z, Chen Y, Zhang R, et al. c-jun N-terminal kinase - c-jun pathway transactivates Bim to promote osteoarthritis. *Can J Physiol Pharmacol*. 2014;92(2):132-139. doi:10.1139/cjpp-2013-0228
- Iezaki T, Ozaki K, Fukasawa K, et al. ATE3 deficiency in chondrocytes alleviates osteoarthritis development. *J Pathol*. 2016;239(4):426-437. doi:10.1002/path.4739

57. Hoppstädter J, Ammit AJ. Role of Dual-Specificity Phosphatase 1 in Glucocorticoid-Driven Anti-inflammatory Responses. *Front Immunol.* 2019;10:1446. doi:10.3389/fimmu.2019.01446
58. Choi Y, Yoo JH, Lee Y, Bae MK, Kim HJ. Calcium-Phosphate Crystals Promote RANKL Expression via the Downregulation of DUSP1. *Mol Cells.* 2019;42(2):183-188. doi:10.14348/molcells.2018.0382
59. Tu M, Yang M, Yu N, et al. Inhibition of cyclooxygenase-2 activity in subchondral bone modifies a subtype of osteoarthritis. *Bone Res.* 2019;7(1):29. doi:10.1038/s41413-019-0071-x
60. Fei J, Liang B, Jiang C, Ni H, Wang L. Luteolin inhibits IL-1 β -induced inflammation in rat chondrocytes and attenuates osteoarthritis progression in a rat model. *Biomed Pharmacother.* 2019;109:1586-1592. doi:10.1016/j.biopha.2018.09.161
61. Zeng GQ, Chen AB, Li W, Song JH, Gao CY. High MMP-1, MMP-2, and MMP-9 protein levels in osteoarthritis. *Genet Mol Res.* 2015;14(4):14811-14822. doi:10.4238/2015.November.18.46
62. Akesson G, Malmend CJ. A Role for Soluble IL-6 Receptor in Osteoarthritis. *J Funct Morphol Kinesiol.* 2017;2(3):27. doi:10.3390/jfmk2030027
63. Latourte A, Cherifi C, Maillot J, et al. Systemic inhibition of IL-6/Stat3 signalling protects against experimental osteoarthritis. *Ann Rheum Dis.* 2017;76(4):748-755. doi:10.1136/annrheumdis-2016-209757
64. Haseeb A, Ansari MY, Haqqi TM. Harpagoside suppresses IL-6 expression in primary human osteoarthritis chondrocytes. *J Orthop Res.* 2017;35(2):311-320. doi:10.1002/jor.23262
65. Orita S, Ishikawa T, Miyagi M, et al. Percutaneously absorbed NSAIDs attenuate local production of proinflammatory cytokines and suppress the expression of c-Fos in the spinal cord of a rodent model of knee osteoarthritis. *J Orthop Sci.* 2012;17(1):77-86. doi:10.1007/s00776-011-0175-7
66. Tang H, Cheng Z, Ma W, et al. TLR10 and NFKBIA contributed to the risk of hip osteoarthritis: systematic evaluation based on Han Chinese population. *Sci Rep.* 2018;8(1):10243. doi:10.1038/s41598-018-28597-2
67. Chen H, Ni Q, Li B, Chen L. Identification of differentially expressed genes in synovial tissue of osteoarthritis based on a more robust integrative analysis method. *Clin Rheumatol.* 2021;40(9):3745-3754. doi:10.1007/s10067-021-05649-z
68. Yatsugi N, Tsukazaki T, Osaki M, Koji T, Yamashita S, Shindo H. Apoptosis of articular chondrocytes in rheumatoid arthritis and osteoarthritis: correlation of apoptosis with degree of cartilage destruction and expression of apoptosis-related proteins of p53 and c-myc. *J Orthop Sci.* 2000;5(2):150-156. doi:10.1007/s007760050142

Supplementary Information

Table S1. GO Enrichment Result

ONTOLOGY	ID	Description	GeneRatio	p.adjust	Count
BP	GO:0050727	regulation of inflammatory response	15/120	2.45E-05	15
BP	GO:0001933	negative regulation of protein phosphorylation	15/120	3.39E-05	15
BP	GO:1901342	regulation of vasculature development	15/120	3.39E-05	15
BP	GO:0042326	negative regulation of phosphorylation	15/120	5.95E-05	15
MF	GO:0048018	receptor ligand activity	12/119	0.003596	12
MF	GO:0030546	signaling receptor activator activity	12/119	0.003596	12
CC	GO:0032023	collagen-containing extracellular matrix	11/120	0.005909	11
MF	GO:0005539	glycosaminoglycan binding	10/119	0.000387	10
MF	GO:0005125	cytokine activity	10/119	0.000387	10
MF	GO:0005126	cytokine receptor binding	9/119	0.003596	9
MF	GO:0001664	G protein-coupled receptor binding	9/119	0.004689	9
MF	GO:0140287	DNA-binding transcription factor binding	9/119	0.0126	9
BP	GO:1990888	response to chemokine	8/120	3.42E-05	8
BP	GO:1990889	cellular response to chemokine	8/120	3.42E-05	8
BP	GO:0096754	detoxification	8/120	0.000253	8
BP	GO:0002687	positive regulation of leukocyte migration	8/120	0.000266	8
BP	GO:0042542	response to hydrogen peroxide	8/120	0.000308	8
BP	GO:0034614	cellular response to reactive oxygen species	8/120	0.000758	8